

Bio-material solvents for Inkjet printing of liquid-exfoliated Graphene/MoS<sub>2</sub> compositesChien Mau Dang<sup>1</sup>, Dung My Thi Dang<sup>1</sup>, LE Thi Minh Chanh<sup>1</sup>, Fatemeh Mollaamin<sup>1</sup>, Majid Monajjemi<sup>1,2,\*</sup><sup>1</sup>Institute for Nanotechnology (INT), Vietnam National University - Ho Chi Minh City (VNUHCM), Ho Chi Minh City, Vietnam<sup>2</sup>Department of chemical engineering, Central Tehran Branch, Islamic Azad University, Tehran, Iran\*corresponding author e-mail address: [Maj.monajjemi@iauctb.ac.ir](mailto:Maj.monajjemi@iauctb.ac.ir)

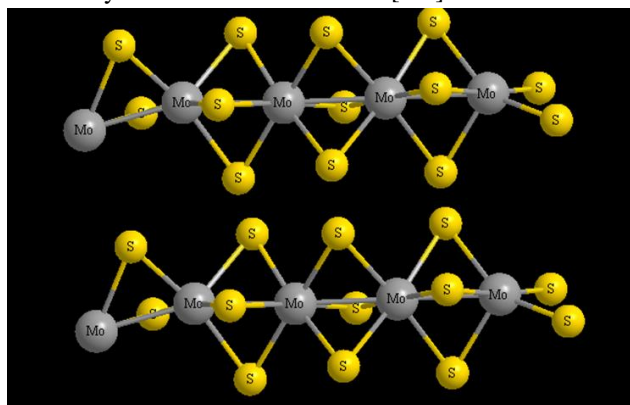
## ABSTRACT

The biologically derived materials are a cost effective and environmentally benign for using an inkjet deposition of liquid exfoliation. MoS<sub>2</sub> and Graphite can be easily exfoliated in a liquid media to extract individual layers. In this work, we exhibited building van der Waals hetero-structures based on Graphene/MoS<sub>2</sub>, 2D blocks with structures of layer-by-layer stacking in viewpoint of surfactant exfoliation with several suitable of biologically derived materials using inkjet deposition technologies. This simulation indicates that Graphene is a suitable substrate for MoS<sub>2</sub> growth towards generating the Graphene/MoS<sub>2</sub> hetero-structures with non-bonded or van der Waals interactions. In this study, we have shown the sulfonic groups in the cation surfactants are most effective for any dispersion in the LPE process of Graphite/MoS<sub>2</sub>. Moreover, the IONIC surfactants have excellent efficiencies compare to those non-ionic or zwitterion structures. Usually, these sequences might be suggested for any dispersion in the LPE processing as cation>anion>zwitterion>nonionic.

**Keywords:** MoS<sub>2</sub>, TMD, thin films, inkjet printing, industrial printing, 2D inks, liquid exfoliation, Graphene.

## 1. INTRODUCTION

The synthesis and production of 2D materials such as Graphene are much important for industrial and research centers. Printed electronics devices are based on novel techniques including several advantages such as the low-cost production of large-area devices, where fundamental need can be seen [1-3]. Developing methods to produce high-purified exfoliated nano-thin films are important in new worlds. The liquid-based exfoliation (LBE) of nano-sheets in biopolymers solvents are one of the most important ways for these kind activities [4-7].



**Scheme 1:** MoS<sub>2</sub>, the most common metal dichalcogenide, adopts a layered structure.

Metal dichalcogenide has the general formula as the “XY<sub>2</sub>”, where X is a transition metal and Y is one of the elements from 6A groups in Mendeleev table (S, Se, Te). They are unclear diamagnetic solids, insoluble in many of solvents along with a strong semiconducting property. Their electronics and orbitals structures are generally have been classified as derivatives of X<sup>4+</sup>, where X<sup>4+</sup> = Ti<sup>4+</sup> (d<sup>0</sup>), V<sup>4+</sup> (d<sup>1</sup>), Mo<sup>4+</sup> (d<sup>2</sup>). TiS<sub>2</sub> was investigated in cathode for the secondary battery because of its ability to reversibly undergo intercalation by lithium [3, 4 and 7].

MoS<sub>2</sub> is the subject of many thousand publications where mainly is ore of molybdenum so called molybdenite (scheme 1). Nano-sheet thin films through a liquid dispersion can be simulated to produce 2D inks for using inkjet printing. Recently, the suitable of layered materials such as molybdenum disulfide (MoS<sub>2</sub>) is widely used for printed electronics devices [8-12]. Amazing group's materials that might be important in printed electronics devices are 2D-materials such as Graphene and transition metal dichalcogenide (TMD) which MoS<sub>2</sub> is one of the important examples of such TMD semiconductors as a non-toxic semiconductor [13,14].

Moreover, the electron dynamism of the layered semiconductors, making them a perfect replacement within high-performances materials as a suitable semiconductor in printed electronics. The MoS<sub>2</sub> [8, 11, 13] is a simplest and powerful semiconductor material which is also appropriate for both solution printing (coating) & environmentally benign [15-17]. The mechanical behavior of such layered materials (MoS<sub>2</sub>), make them suited molecules for electronics processing practically. The simulation investigated by this work could be applied for exfoliating in several types of 2D sheets in organic liquids which contains two exfoliation phases including (1): mechanical exfoliation utilizing sandpapers from the bulk powders, and (2): the liquid dispersion and sonication over the nano sheets [18-20]. The highest electrons motilities of those TMD materials such as MoS<sub>2</sub> in comparison with other printable semiconductors (the organic molecules), make applications using thin films of layered materials as very interesting. General applications can be found for those materials in the fields of gas detector, catalysis, energies storages and solar cell systems, but so far, the main body of work has focused on single nanosheets. By this simulation, it has been suggested the simplest ways in ink developing to drop formation, break-of at the nozzle and consequently the printing qualities [21]. Inkjet printing is a material-patronizing deposition method used

for liquid phase composition and the inks material generally is a solute dissolved for dispersion in the solvents [22, 23]. The mechanisms basically contain two steps, one the rapid rejection of ink in a cell via a nozzle and second the quasi-adiabatic reduction of the cell volume through piezoelectric reactions. Chamber cells filled with liquids are compressed due to an external voltage and quickly make up a shock-wave, which causes the liquid dropping and ejecting from the nozzle [24, 25].

Under gravity forces, the drops fall down and their motion spread in two dimensions while the tension aided flow along the surfaces and then the drops dry via solvent vaporization [26-28]. Recent investigation exhibit which drops spreading and the last printed situation completely depends on the viscosity of solvents and the viscosity is a function of the polymer's molar mass and also a function of the polymer concentration. Although there are wide-developing by metallic and organic printed electronic ink's devices, there are still a necessary improving or developing of

novel inks based on semiconductors and stable compounds such as TMD which has a suitable jetting position for delivering a good within high quality of printing [29, 30]. Therefore the suitable way is using of a novel approach via the liquid-based exfoliation (LBE) application of a nanosheet in several solvents, which is the first step of obtaining thin films. Although the process of exfoliating Graphene layers from a pristine graphite crystal is the simplest exfoliation method for the micromechanical division to separate the layers from MoS<sub>2</sub>, limiting its application to devices that employ single nanosheets of 2D materials [14-24]. Scalable exfoliation approaches within higher efficiency has investigated by several researchers [15-18], and one type of theme has been expanded by Coleman *et al.* [20]. Based on one of our works [31], we used the exfoliation method of MoS<sub>2</sub> dispersions in various organic solvents such as various surfactants and several aromatic compounds [31].

## 2. EXPERIMENTAL SECTION

**2.1. Liquid-Phase Exfoliation (LPE).** MoS<sub>2</sub> and Graphite can be easily exfoliated in a liquid media to extract individual layers. The LPE mechanism usually consists of three steps of (1) dispersion in a solvent, (2) exfoliation in a solvent, and (3) purification. MoS<sub>2</sub> mono layer and also Graphene flakes can be produced by surfactants free exfoliation from graphite or MoS<sub>2</sub> crystal layers via a chemical wet dispersion processing in several organic solvents. After exfoliation, the solvent-layer interaction manages the balancing of the inter-sheet attractive forces. In this work different solvents have been considered for simulating the MoS<sub>2</sub> exfoliation. In order to determine exfoliation yields it is necessary to fit the exfoliated MoS<sub>2</sub> materials providing both qualitative and quantitative data. For any further results and discussion; QM/ MM calculations have been done for solvents versus MoS<sub>2</sub> layers with different mole ratios are important for estimating the concentration of dispersion.

Although the van der Waals attractions between adjacent layers are weak and unstable, the attraction is tight enough for making complete exfoliation into individual layer by layer challenging. Obviously, a single-layer of MoS<sub>2</sub> sheets through exfoliations have been produced via surfactants media especially anion surfactants. For the large-scale production of MoS<sub>2</sub> layers, many unsuccessful attempts have been made with several solvents because successful exfoliations need the conquering of the van der Waals attractions among the adjacent MoS<sub>2</sub> layers. One of the main important methods for reducing the strength of the van der Waals forces is liquid plunging, where the potential energies among adjacent layers have been contributed by dispersive London forces, which in the media of a solvent are significantly reduced with respect to vacuum.

It is notable that interfacial tension plays an important role during plunging of the solid surfaces in solvent media. If the interfacial tension between solids and liquids are much higher, there is weak dispersion ability in the solids inside the liquids. In the case of MoS<sub>2</sub>, if the interfacial tension is high, the layers tend to cohere to each other and the cohesion between them is higher. Commonly, water has more use for the solid surfaces energies, because surfaces tensions of dispersed phases of water are 21.5 mJ/ m<sup>2</sup> and its polar phase is 52.0 mJ/ m<sup>2</sup>. Solvents with high surfaces tensions are a suitable solvent for these kind dispersions of MoS<sub>2</sub>. By this work, several solvents including cation, anion, zwitterion and nonionic forms such as 6, 8-Dihydroxyle-1, 3, 6, 8-pyrenedisulfonic acid, 1-Pyrene carboxylic acid, N-methyl-2-pyrrolidone (NMP), N, N-dimethyl-form amide and Ortho-dichlorobenzene (o-DCB) have been simulated, in Figs.(1-4).

**2.2. Surfactant & Liquid media in MoS<sub>2</sub> and graphite exfoliation.** Surfactants can promote the exfoliation of MoS<sub>2</sub> into one layer structure, especially during the high energies of adsorption on the MoS<sub>2</sub>, and especially being higher than the one of the surfactant molecule interacting with those surfaces. The use of ion surfactant might be also stabilizing exfoliated structure in organic solvents such as DMSO, Ethanol, and Methanol.

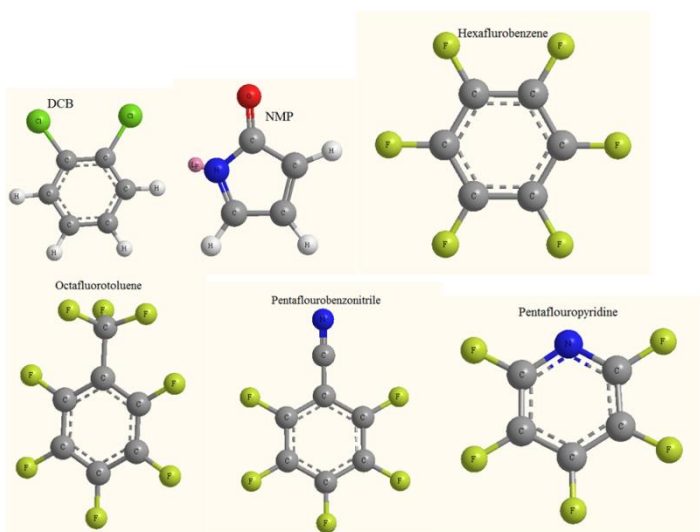


**Fig. 1:** Solvents used as liquid media in the exfoliation process including: N-methyl-2-pyrrolidone (NMP), dichlorobenzene (DCB) and per-fluorinated aromatic solvents for colloidal dispersions.

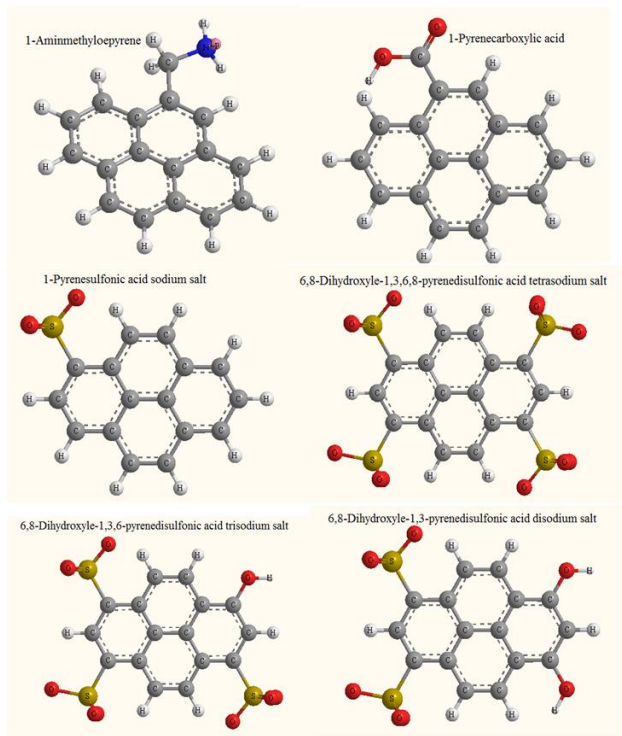


**Fig. 2:** Pyrene derivatives used as surfactants in the process of LPE of MoS<sub>2</sub> and Graphene for Inkjet deposition of liquid-exfoliated

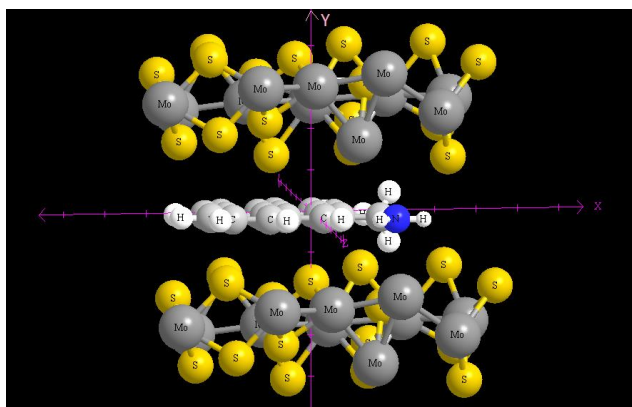


**Fig. 3:** 1-Aminmethylpyrene between two layers of MoS<sub>2</sub>

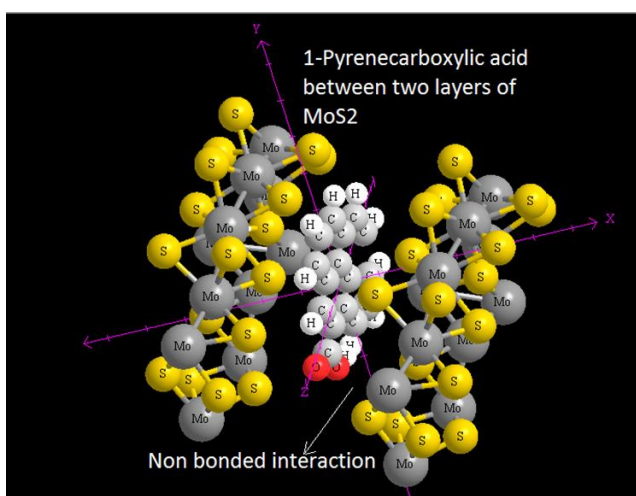


**Fig. 4:** 1-Pyrenecarboxylic acid between two layers of MoS<sub>2</sub>

Water is a natural matter as an aqueous dispersion due to its non-toxicity that opens the perspective for the materials for biomedical applications. Although the exfoliation of MoS<sub>2</sub> in

water is exclusively challenging due to the hydrophobic nature of the sheets, such a challenge can be overcome by using surfactants. Surfactant individually may stabilize the nano-sheets via the mechanisms of semi-micelles, as exhibited in recent research [32, 33]. Sodium dodecyl sulfate (SDS) is one of the most important surfactants for exfoliation and its charging which could also influence the net charges densities on the unit surface (as instant for ionic surfactant) which has been applied in our work. Furthermore, adding surfactant is needed for controlling the surfaces tension of the inkjet inks that is a majority subject during dropping formation at the inkjet printing nozzles. One of the important parameters for 2D inks is electrophoretic mobility or zeta potential which can evaluate the stability of the surface through estimating the surfaces charges of a nano-sheet via electrophoretic mobility properties. Electrophoresis's mobility is an evaluation of the zeta potentials. The measurements are performed via estimating the rates of diffusion for the surfaces charges when the electrical fields are applied. These rates of diffusion are related to the strengths of electrical fields. The electrophoresis's mobility measures inter-Fe<sup>II</sup>-metric's laser technique which enabled the calculations of electrophoresis's mobility for estimating zeta potential.

Surfactants allow exfoliated sheets for remaining suspended due to their p-p stacking interactions with MoS<sub>2</sub>, the polycyclic aromatics hydrocarbons show suitable behavior in this matter.

Pyrene derivative has been applied by various functions for stabilizing MoS<sub>2</sub> dispersion.

The number of MoS<sub>2</sub> and Graphene layers can be evaluated via the experimental activities (Rayleigh spectroscopy) [36], while the theoretical calculation can be estimated through an ab-initio method. Although this kind of approaches only works for some exfoliated samples, does not provide other electronics information. Raman spectroscopy can be applied to all Graphene samples. Moreover, it is able to identify by-products, damages, electronics perturbation introduced, structural and functional, chemical modifications during the preparation, processing or placement of both MoS<sub>2</sub> and Graphene. As a result, a Raman spectrum is an important tool for comparing some samples in viewpoint of qualities, controlling. Recently, there are significant approaches and methods for understanding the Raman spectroscopies in MoS<sub>2</sub> exfoliation, such as doping, oxidation, electrical mobility. Commonly, Raman spectroscopies are used for determining exfoliation yields to parallel confirmation with results of AFM or TEM.

The distances among stacked parallel MoS<sub>2</sub> layers in bulk structures have been calculated via DFT methods. Although the van der Waals attractions among adjacent layers are not strong enough, the attractions are strong for making complete exfoliation into individual layers challenging. One of the most important methods for reducing the strength of the van der Waals attractions is liquid plunging, where the potential energies among adjacent layers are contributed by dispersion London interactions, which in the media of a solvent are extremely reduced with respect to vacuum. It has been found that interfacial tension plays a key role

when the solid surfaces such as MoS<sub>2</sub> is plunged in a liquid medium or surfactants [37]. If the interfacial tensions among solids are high, there is a poor dispersion in the liquids [37]. In the case of graphitic flakes, if the interfacial tension is high, the flake tends to cohere to each other and the cohesion between them is high. Solvents including surfaces tensions are the best solvents for the dispersion of MoS<sub>2</sub> and also graphitic flakes since they minimize the interfacial tension between solvent and layers.

In this work, several solvents including N-methyl-2-pyrrolidone (NMP), dichlorobenzene (DCB) and per fluorinated aromatic have been used as an index and some other solvents have been compared to these indexes Figs.(2-4).

**2.3. Thermal inkjet (TIJ) & Piezo technology.** Actually the TIJ, also famous as a bubble jet which can be illustrated as a current for using a heating element inside the printing which is an attaché to the ink. As results, a temperature between 300 - 350 °C is suitable for the simulation. A medium bubble of vapor might be formed due to the higher vapor's occupation compare to the liquid consequently the pressure inside the ink chamber is increased and the ink is ejected from the nozzle. The retracting meniscus breaks the ligament, and a drop is separated. Basically, the heating element starts to cool down, and the bubble will collapse. The whole processing of a bubble construction and also collapsing take from 2.5 to 10.5 μs and the ink should have a volatile component, which is one disadvantage of these kind technologies [34, 35]. In piezo method, the ink ejects through the deformation of the piezo material during the electrical field appearing. Which cause suddenly, changing into the inks of the chamber to generate a waves propagate. Via the ink, these pressures have to overcome a few forces for enabling dropping formation and ejection.

**2.4. Theoretical background.** TEM, AFM, and SEM are the normal methods for studying the LPE and determining the electron densities profile across the adsorption onto those sheets. The derivation of these kind electron densities profiles requires knowledge of both the X-ray reflections and their corresponding phase angles. Although the amplitudes can be quickly determined from a diffraction patterns, the phases of that reflection cannot be directly observed.

Moreover, due to the difficulties in estimating absolute intensities, the profiles are seldom calculated on the relative electrons densities scales. The lack of absolute scales has been often greatly hindered the interpretation of the layers, particularly with regards to the distribution of the protein molecules.

In this work, a new method of step-function models of the electron densities in the composition of the layers has been introduced which mainly focused on the electron densities of the systems when the layers of Graphene or MoS<sub>2</sub> have been created one by one via LPE. The electron densities have been defined as:

$$\rho(r) = \eta_i |\varphi_i(r)|^2 = \sum_i \eta_i \left| \sum_l C_{l,i} \chi_l(r) \right|^2 \quad (1)$$

Where  $\eta_i$  occupation number of orbitals,  $C$  is coefficients matrixes in which the element of the  $i_{th}$  row and  $j_{th}$  column corresponds to the expansion coefficient of orbital  $j$  with respect to basis function  $i$ . Bader [38] has exhibited that the

regions with larger ELF must have a large number of Fermi-hole integration.

Becke and coworkers have been mentioned that spherically averaged spins probability have a direct correlation with the Fermi hole and then shown the electron localization function (ELF) [39] as follows:

$$ELF(r) = \frac{1}{1+[D(r)/D_0(r)]^2} \quad (2) \text{ where}$$

$$D(r) = \frac{1}{2} \sum_i \eta_i |\nabla \varphi_i|^2 - \frac{1}{8} \left[ \frac{|\nabla \rho_\alpha|^2}{\rho_\alpha(r)} + \frac{|\nabla \rho_\beta|^2}{\rho_\beta(r)} \right] \quad (3) \text{ and}$$

$$D_0(r) = \frac{3}{10} (6\pi^2)^{\frac{2}{3}} [\rho_\alpha(r)^{\frac{5}{3}} + \rho_\beta(r)^{\frac{5}{3}}] \quad (4)$$

In a close-shell system, since  $\rho_\alpha(r) = \rho_\beta(r) = \frac{1}{2}\rho$ ,  $D$  and  $D_0$  terms can be simplified as  $D(r) = \frac{1}{2} \sum_i \eta_i |\nabla \varphi_i|^2 - \frac{1}{8} \left[ \frac{|\nabla \rho|^2}{\rho(r)} \right]$  and  $D_0(r) = \frac{3}{10} (3\pi^2)^{\frac{2}{3}} \rho(r)^{\frac{5}{3}}$ .

Savin *et al.* have reinterpreted ELF based on kinetic energies, [40] which would make ELF corresponds to the Kohn-Sham DFT wave-function. They exhibit that  $D(r)$  reveals the excess kinetic energies density caused by Pauli repulsion, while  $D_0(r)$  can be considered as Thomas-Fermi kinetic energy densities. Obviously, the ELF is within the range of [0, 1] and so a large ELF value means that electrons are greatly localized, indicating that covalent bonds, i.e. a lone pair or inner shells of the atoms are involved. ELF has been widely used for a wide variety of systems, such as exfoliation methods.

It might be noted that there is a deficiency of ELF, sometimes with  $r$  going beyond from the molecular boundary where the  $D(r)$  decreases quicker than  $D_0(r)$ . For removing this problem, Multi-wfn [41] automatically adds a minimal value of 10<sup>-5</sup> to  $D(r)$ . This treatment does not really affect the ELF value in interesting regions, in which case, the real kinetic energies terms in  $D(r)$  are replaced by Kirzhnits type second-order gradient expansion that is:

$$\frac{1}{2} \sum_i \eta_i |\nabla \varphi_i|^2 \approx D_0(r) + \frac{1}{72} \frac{|\nabla \rho|^2}{\rho(r) + \frac{1}{6} \nabla^2 \rho(r)} \quad (5)$$

Therefore the ELF's are totally independent of the wave-functions and might be used for analyzing electron densities from X-rays diffractions data. Another function similar to ELF's is called the localized orbital locator (LOL) which is used for locating high localization regions. This function is defined by Schmider and Becke

$$LOL(r) = \frac{\tau(r)}{1+\tau(r)}, \text{ where } \tau(r) = \frac{D_0(r)}{\frac{1}{2} \sum_i \eta_i |\nabla \varphi_i|^2} \quad (6)$$

$D_0(r)$ , For spin-polarized systems are defined in the same root compared to that in ELF. Actually, the chemically significant regions that highlighted by LOL and ELF are generally qualitatively comparable, while Jacobsen pointed out that LOL conveys a clearer and more decisive picture compared to ELF, [41]. However, LOL can also be interpreted in terms of the localized orbital. Smaller or larger values of LOLs are commonly appeared in the boundary region of localized orbitals due to the small gradient of orbital wave-function in this area respectively. This simulation have been done based on our previous works [42-59].

### 3. RESULTS SECTION

It has been exhibited the exfoliation of MoS<sub>2</sub> (Figs 5, 6) as the same graphite can be achieved by surfactants, polar and non-covalent functionalization using several solvents such as carboxylic acid (ACA) which possess remarkable electronic properties. This work has been focused on the surfactant-MoS<sub>2</sub> layers and this strategy can be used in other media of surfactants including cation, anion, non-ionic and zwitterion. As it has been exhibited in the tables 3-6; the electrical characters in the electron density distributions indicate the situation of exfoliation for each layer. The energy densities and Potential energies densities for several solvents were calculated and fitted from the solvent-MoS<sub>2</sub> for all simulations. Based on equals1-5 the larger of electron localizations are in the surfactants with higher polar sides including nonpolar chains. In the tables (3-6) several different ionic surfactants such as anions, cations, non-ions and zwitterions are listed and as it can be seen, water is not recommended as a suitable media for exfoliation of Graphene but it is suitable for MoS<sub>2</sub> (Fig.6) because the presence of H<sub>2</sub>O molecules at the interface with a dielectric around 78.8 can enhance charges trapping mechanism for Graphene (not for MoS<sub>2</sub>) layers. Therefore, application of an organic solvent (tables 4-6) for exfoliating has been recommended.

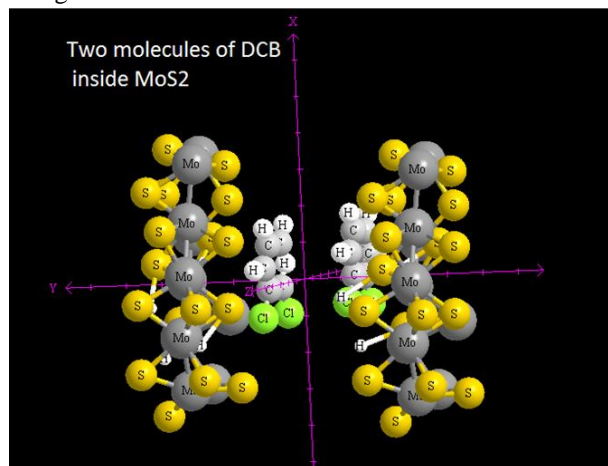


Fig. 5: Two molecules of DCB between two layers of MoS<sub>2</sub>

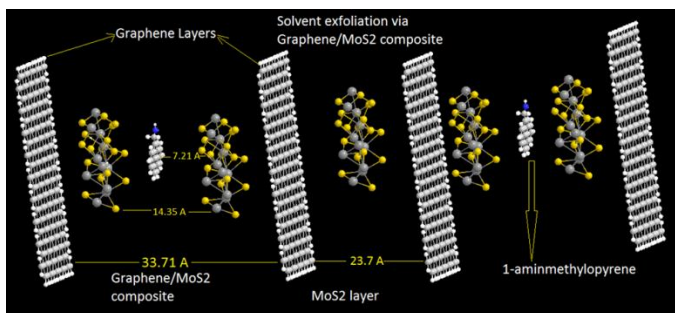


Fig. 6: Solvent exfoliation via Graphene/MoS<sub>2</sub> Composite

Table 1: G (r), K (r), V (r), H (r), ELF, LOL, LIE and Total ESP for MoS<sub>2</sub>.

Sulfur number	G (r)	K (r)	V (r)	H (r)	ELF	LOL	Average (LIE)	Total ESP kcal/mol
Mo	0.2419	-0.3193	-0.3193	0.3193	0.2226	0.1481	0.8218	0.6152
S(1)	0.2273	-0.2024	-0.1764	0.2024	0.2152	0.1542	0.8309	0.6143
S(2)	0.2792	-0.2104	-0.2655	0.2104	0.1521	0.1438	0.8312	0.6174

Table 2: G (r), K (r), V (r), H (r), ELF, LOL, LIE and Total ESP for 6,8-Dihydroxyle-1,3,6-pyrenedisulfonic acid tri-sodium salt

Sulfur number	G (r)	K (r)	V (r)	H (r)	ELF	LOL	Average (LIE)	Total ESP kcal/mol
Mo (1)	0.2201	-0.2323	-0.1849	0.2323	0.3027	0.1605	0.7293	0.6188
S (1)	0.2283	-0.2323	-0.1967	0.2323	0.2452	0.1474	0.8265	0.6166
S (2)	0.2174	-0.2023	-0.1963	0.2023	0.3055	0.1742	0.8456	0.6144

Table 3: Low and Medium dispersions Zwitterion surfactants

Surfactant	Ionic	Chemical formula	Molar (g/mol) mass	Dispersions Predication Graphene/MoS <sub>2</sub>
Cocamidopropyl betaine (CAPB)	Zwitter	C <sub>19</sub> H <sub>38</sub> N <sub>2</sub> O <sub>3</sub>	342.52	M
CHAPS detergent	Zwitter	C <sub>32</sub> H <sub>58</sub> N <sub>2</sub> O <sub>7</sub> S	614.88	L
Sodium lauroamphoacetate	Zwitter	C <sub>18</sub> H <sub>34</sub> N <sub>2</sub> NaO <sub>3</sub>	349.47	L
Lauroamidopropyl betaine	Zwitter	C <sub>19</sub> H <sub>38</sub> N <sub>2</sub> O <sub>3</sub>	342.52	L

Table 4: Medium, high and Low dispersions anion surfactant

Surfactant	Ionic	Chemical formula	Boiling point	Density g/cm <sup>3</sup>	Solubility	Molar (g/mol) mass	Melting point	Dispersions Predication Graphene/MoS <sub>2</sub>
Dodecane	-	C <sub>12</sub> H <sub>26</sub>	Melting point=153 to 157 °C	1.1	1 in 70 parts mg/mL in water	444.56		H
Ammonium dodecyl sulfate	-	C <sub>12</sub> H <sub>25</sub> NO <sub>4</sub> S	418°C	1.02		283.43		H
Perfluorobutanesulfonic acid (PFBS)	-	C <sub>4</sub> HF <sub>9</sub> O <sub>3</sub> S	211 °C			300.10	76 to 84 °C	Low
Sodium 1,4-bis(2-ethylhexoxy)-1,4-di-oxobutane-2-sulfonate	-	C <sub>20</sub> H <sub>41</sub> NaO <sub>5</sub> S		1.1	1 in 70(H <sub>2</sub> O)	444.56		M
Perfluorobutanesulfonic acid	-	C <sub>4</sub> HF <sub>9</sub> O <sub>3</sub> S	211°C			300.1	76°C	H
Heptadecafluorooctanoic acid	-	C <sub>8</sub> HF <sub>17</sub> O <sub>2</sub>			polar organic solvents	464.08	59°C	H
1,1,2,2,3,3,4,4,5,5,6,6,7,7,8,8,8Hepta dicalcyl-octane sulfonic acid	-	C <sub>8</sub> H <sub>17</sub> O <sub>3</sub> S	133°C			500.13		H
Pentadecafluorooctanoic acid	-	C <sub>8</sub> HF <sub>17</sub> O <sub>2</sub>	189°C	1.8	9.5 g/L In H <sub>2</sub> O	414.07	40°C	H
Sodium dodecyl sulfate (SDS)	-	NaC <sub>12</sub> H <sub>25</sub> SO <sub>4</sub>		1.01		288.3	206 °C	H
Potassium dodecyl sulfate	-	C <sub>12</sub> H <sub>25</sub> KO <sub>4</sub> S				304.49		H
Sodium lauryl sulfate	-	NaC <sub>12</sub> H <sub>25</sub> SO <sub>4</sub>		1.01		288.37	206°C	H
Sodium dodecyl benzenesulfonate	-				20%in water	348.48		H
Sodium dodecanoate	-	C <sub>12</sub> H <sub>23</sub> O <sub>2</sub> Na		1.102		222.3	244°C	M
Perfluorooctanesulfonic acid	-	C <sub>8</sub> HF <sub>17</sub> O <sub>3</sub> S	133 °C			500.13		M

Table 5: Medium and high dispersions cation surfactant

Surfactant	Ionic	Chemical formula	Boiling point	Density g/cm <sup>3</sup>	Solubility	Molar (g/mol) mass	Melting point	Dispersions Predication Graphene/MoS <sub>2</sub>
Cetrimonium bromide CTAB	+	[(C <sub>16</sub> H <sub>33</sub> N(CH <sub>3</sub> )) <sub>3</sub> Br]	Micelle point= 30°C			364.45 g/mol	237 to 243 °C	H
Benzethonium chloride	+	C <sub>21</sub> H <sub>42</sub> ClNO <sub>2</sub>		0.98	40 g dm <sup>-3</sup> in water	448.09	244°C	H
5-Bromo-5-nitro-1,3-dioxane	+	C <sub>6</sub> H <sub>8</sub> BrNO <sub>4</sub>			Insoluble in water	212.0	60°C	M
Hexadecyltrimethylammoniumbromide	+	C <sub>19</sub> H <sub>41</sub> BrN				364.45	237.0°C	H
N,N-Dimethyl-N-octadecyldecadecan-1-aminiumchloride	+	C <sub>18</sub> H <sub>40</sub> ClN				586.52	25°C	M
Cetylpyridinium chloride (CPC)	+	C <sub>21</sub> H <sub>33</sub> ClN				339.9 g/mol	77 °C	Low
N,N'-tris(2-hydroxyethyl)-N'-octadecylpropane-1,3-dithiame dihydrochloride	+	C <sub>27</sub> H <sub>60</sub> F <sub>2</sub> N <sub>2</sub> O <sub>2</sub>				498.77		H
Benzalkonium chloride	+			0.98	very soluble			M
Tetramethylzanium hydroxide	+	C <sub>4</sub> H <sub>13</sub> NO		1.015	decomposes	91.15	67°C	H

The MoS<sub>2</sub> inks were printed within the gaps of the Graphene electrodes a few (50-70 μm) overlapping are needed for ensuring a complete filling of the gaps and contacts with the Graphene. These electrode setups were used to the photoconductive properties of exfoliated MoS<sub>2</sub>. In this work, we exhibited building van der Waals hetero-structures based on Graphene/MoS<sub>2</sub>, 2D blocks with structures of layer-by-layer stacking is suitable hetero-structures construction for Inkjet deposition. However, interfacial contamination would be a major factor to be considered. By this method, it has been illustrated the advantages of reduce adsorbents on individual layer. This simulation exhibits that Graphene is a suitable substrate for MoS<sub>2</sub>

growth towards generating the Graphene/MoS<sub>2</sub> hetero-structures with non-bonded or van der Waals interactions.

**Table 6:** Low and medium dispersions non-ionic surfactants

Surfactant	Ionic	Chemical formula	Boiling point	Density g/cm <sup>3</sup>	Solubility	Molar (g/mol) mass	Melting point	Dispersion Prediction Graphene/MoS <sub>2</sub>
Triton X-100	Non	C <sub>18</sub> H <sub>32</sub> O <sub>6</sub> C <sub>2</sub> H <sub>4</sub> O λ <sub>n</sub> (n=9-10)	270°C	1.07	Soluble in water	647	6°C	L
Polysorbate 80	Non	C <sub>64</sub> H <sub>122</sub> O <sub>24</sub>	100°C	1.06	Soluble in ethanol, water, ethylacetate, methanol, toluene	1310		M
Stearyl alcohol	Non	C <sub>18</sub> H <sub>37</sub> O	210°C	0.812	1.1 x 10 <sup>-2</sup> mg/L in water	270.49	59.4°C	L
Sorbitan tristearate	Non	C <sub>58</sub> H <sub>110</sub> O <sub>9</sub>				963.54		L
Decyl glucoside	Non	C <sub>16</sub> H <sub>32</sub> O <sub>5</sub>				320.43		L
Lauryl glucoside	Non	C <sub>18</sub> H <sub>36</sub> O <sub>5</sub>				348.48		M
Oleyl alcohol	Non	C <sub>19</sub> H <sub>39</sub> O	330.0°C	0.845	Insoluble in water	268.47	13.0°C	M
n-Octyl β-D-thiopyranoside	Non	C <sub>14</sub> H <sub>28</sub> O <sub>5</sub> S				308.43		L
Nonoxynol-9	Non	C <sub>19</sub> H <sub>39</sub> O <sub>10</sub>				616.83		
Cetyl alcohol	Non	C <sub>22</sub> H <sub>44</sub> O	344.0°C	0.811	Very soluble in ether, benzene, chloroform, acetone	242.45	49.3°C	

MoS<sub>2</sub> nano-flake on the Graphene sheet is hexagonal, with crystal size ranging from 100-1000 nm. Although there is existed a lattice mismatch between Graphene and MoS<sub>2</sub>, the gap could be well accommodated within these hetero-structures. The well conductivities of Graphene in combination with the electronic properties of MoS<sub>2</sub> show a way for developing of Graphene-based nanostructure for inkjet deposition of liquid.

If electrons are completely localized in the Graphene/MoS<sub>2</sub> hetero-structures, then they can be distinguished from the ones outside. As shown in tables 1-2 the sulfur atoms precede the large ELF which is near to the polar side. As the regions which have large electron localization must have large magnitudes of Fermi-hole integration, so these phenomena leads the surfactants towards the polar side with exceeding electrons and nonpolar side with exceeding holes. Based on equations 2- 4, Becke and Edgecombe noted that spherically averaged spin conditional pair probabilities have a direct correlation with the Fermi hole which it is suitable to correspond to our data in table 1-2. ELF reveals is actually a relative localization within the ranges between 0- 1.

A large ELF magnitude indicates the electrons are greatly localized, which means there is a covalent bond, a lone pair or inner shells of the atoms between Graphene/MoS<sub>2</sub> systems.

Based on eq.6, LOL can be interpreted in kinetic energy way as for ELF; however, LOL can also be interpreted in view of the localized orbital. Small LOL value generally appears in the boundary region of localized orbital due to the gradient of orbital wave-function. Although LOL has similar expression compared to ELF, the LOL conveys clearer pictures than ELF. In tables, 1-2 and Figure 7, 8 the ELF, electron density profiles, densities of states, TDOS and PDOS are listed and displayed. Here we have considered the interlayer attraction of the graphite/MoS<sub>2</sub> using OM/MM with ONIOM methods including OPLS and CHARMM force fields to describe the interlayer interactions and the classical mono-polar electrostatic terms. In this study, via the number of layers and volume of graphite/MoS<sub>2</sub>, the estimation of area for the upper and downer (Graphene and MoS<sub>2</sub> respectively) lateral sheets, have been calculated. The layers of surfactants chains give positive amplitudes, which increase quickly so the terminal methyl groups give a narrow region of lower electron density. It is discussable that for graphite/MoS<sub>2</sub> containing a few layers, the different voltages between two layers would relate to several conditions such as non-equilibrium states and dynamic situations

of the coupling among the surfactants and adjacent layers, etc. For Graphite/MoS<sub>2</sub> composition and in the presence of polar solvents or ions surfactants, charges exert forces that can influence the states of the Graphite/MoS<sub>2</sub>; thereby influencing the variable fields causes a variable LPE process.

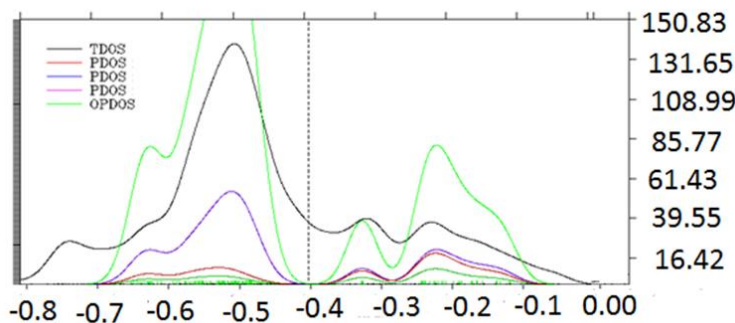


**Fig. 7:** TDOS, PDOS, OPDOS versus energy for Graphene/MoS<sub>2</sub> Composite

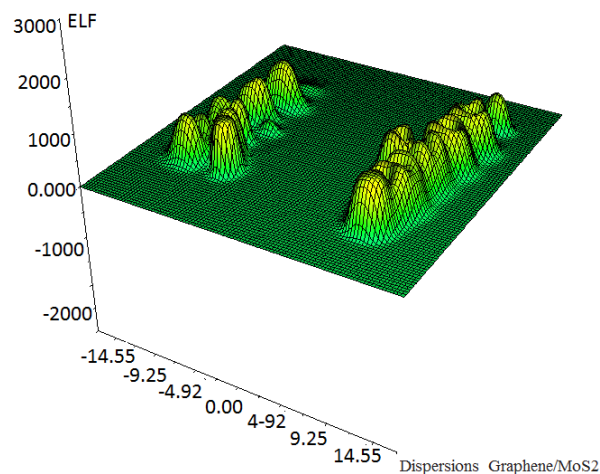


**Fig. 8:** ELF of Graphene/MoS<sub>2</sub> dispersion

In this study, we have shown the sulfonic groups in the cation surfactants are most effective for any dispersion in the LPE process of Graphite/MoS<sub>2</sub>. Moreover, the IONIC surfactants have excellent efficiencies compare to those non-ionic or zwitterion structures. Usually, these sequences might be suggested for any dispersion in the LPE processing as cation > anion > zwitterion > nonionic.

Obviously, the choice of the surfactant might be achieved only through analyzing of exfoliated bio-materials. Especially, using of sodium dodecyl benzene sulfate (SDBS) can be wildly successful. The organic stabilities of exfoliated Graphite/MoS<sub>2</sub> material provided Langmuir–Blodgett (LB) films to be made on various clear substrates, such as glass and quartz, for producing films as both transparent and conducting. By this work, it has been illustrated that porphyrins which are used in our simulations, interact with several carbon materials, such as, graphite and carbon nanotubes, via p-stacking which takes place between their electron-abundant aromatic cores and conjugated surfaces of the carbon materials. Therefore, similar interactions are expected for occurring between Graphene/MoS<sub>2</sub> and Porphyrins biomaterials. Therefore, the electronic properties of MoS<sub>2</sub> show a way for developing of Graphene based nanostructure for inkjet deposition of liquid.

## 4. CONCLUSIONS

Theoretically, it has been exhibited the exfoliation of graphite/MoS<sub>2</sub> can be achieved by surfactants, polar and non-covalent functionalization using bio-solvent materials. The well

conductivities of Graphene in combination with the electronic properties of MoS<sub>2</sub> shows a way for developing of Graphene based nanostructure for inkjet deposition of liquid.

## 5. REFERENCES

- [1] Dimitrakopoulos C.D., Malenfant P.R., Organic thin film transistors for large area electronics, *Advanced Materials*, 14, 99–117, **2002**.
- [2] Søndergaard R.R., Hösel M., Krebs F.C., Roll-to-Roll fabrication of large area functional organic materials, *Journal of Polymer Science Part B: Polymer Physics*, 51, 16–34, **2013**.
- [3] Sun Y., Rogers J.A., Inorganic semiconductors for flexible electronics, *Advanced Materials*, 19, 1897–1916, **2007**.
- [4] Fortunato E., Barquinha P., Martins R., Oxide Semiconductor Thin-Film Transistors: A Review of Recent Advances, *Advanced materials*, 24, 2945–2986, **2012**.
- [5] Nathan A. *et al.*, Flexible electronics: the next ubiquitous platform, *Proceedings of the IEEE*, 100, 1486–1517, **2012**.
- [6] Alharbi F., *et al.*, Abundant non-toxic materials for thin film solar cells: Alternative to conventional materials, *Renewable Energy* 36, 2753–2758, **2011**.
- [7] Cunningham G., Hanlon D., McEvoy N., Duesberg G.S., Coleman J.N., Large variations in both dark-and photoconductivity in nanosheet networks as nanomaterial is varied from MoS<sub>2</sub> to WTe<sub>2</sub>, *Nanoscale*, 7, 198–208, **2015**.
- [8] Li J., Naiini M.M., Vaziri S., Lemme M.C., Östling M., Inkjet Printing of MoS<sub>2</sub>, *Advanced Functional Materials*, 24, 6524–6531, **2014**.
- [9] Li J., *et al.*, A simple route towards high-concentration surfactant-free Graphene dispersions, *Carbon*, 50, 3113–3116, **2012**.
- [10] Li J., *et al.*, Efficient Inkjet Printing of Graphene, *Advanced Materials*, 25, 3985–3992, **2013**.
- [11] Finn D.J., *et al.*, Inkjet deposition of liquid-exfoliated Graphene and MoS<sub>2</sub> nano sheets for printed device applications, *J. Mater.Chem. C*, 2, 925–932, **2014**.
- [12] Novoselov K.S., *et al.*, Electric Field Effect in Atomically Thin Carbon Films, *Science*, 306, 666–669, **2004**.
- [13] Radisavljevic B., Radenovic A., Brivio J., Giacometti V., Kis A., Single-layer MoS<sub>2</sub> transistors, *Nature nanotechnology*, 6, 147–150, **2011**.
- [14] Wang H., *et al.*, Integrated Circuits Based on Bilayer MoS<sub>2</sub> Transistors, *Nano Letters*, 12, 4674–4680, **2012**.
- [15] Wang Q.H., Kalantar-Zadeh K., Kis A., Coleman J.N., Strano M.S., Electronics and optoelectronics of two-dimensional transition metal dichalcogenides, *Nature Nanotechnology*, 7, 11, 699–712, **2012**.
- [16] Chhowalla M. *et al.* The chemistry of two-dimensional layered transition metal dichalcogenide nano sheets, *Nature Chemistry*, 5, 4, 263–275, **2013**.
- [17] Paton K.R., *et al.*, Scalable production of large quantities of defect-free few-layer Graphene by shear exfoliation in liquids, *Nature materials*, 13, 624–630, **2014**.
- [18] Varrla E., *et al.*, Large-Scale Production of Size-Controlled MoS<sub>2</sub> Nano sheets by Shear Exfoliation, *Chemistry of Materials*, 27, 1129–1139, **2015**.
- [19] Jariwala D., Sangwan V.K., Lauhon L.J., Marks T.J., Hersam M.C., Emerging device applications for semiconducting two-dimensional transition metal dichalcogenides, *ACS nano* 8, 1102–1120, **2014**
- [20] Coleman J.N., *et al.*, Two-Dimensional Nanosheets Produced by Liquid Exfoliation of Layered Materials, *Science*, 331, 568–571, **2011**.
- [21] Niu L., *et al.*, Production of Two-Dimensional Nano materials via Liquid-Based Direct Exfoliation, *Small*, 12, 272–293, **2016**.
- [22] Kim S., *et al.*, High-mobility and low-power thin-film transistors based on multilayer MoS<sub>2</sub> crystals, *Nature communications*, 3, 1011, **2012**.
- [23] Mak K.F., Lee C., Hone J., Shan J., Heinz T.F., Atomically Thin MoS<sub>2</sub>: A New Direct-Gap Semiconductor, *Phys. Rev. Lett.*, 105, 136805, **2010**.
- [24] Kuc A., Zibouche N., Heine T., Influence of quantum confinement on the electronic structure of the transition metal sulfide TS<sub>2</sub>. *Phys. Rev. B*, 83, 245213, **2011**.
- [25] Splendiani A., *et al.*, Emerging Photoluminescence in Monolayer MoS<sub>2</sub>. *Nano Letters*, 10, PMID: 20229981, 1271–1275, **2010**.
- [26] Tributsch H., Photoelectrochemical behaviour of layer-type transition metal dichalcogenides, *Faraday Discuss. Chem. Soc.*, 70, 189–205, **1980**.
- [27] Das S., Chen H.Y., Penumatcha A.V., Appenzeller J., High performance multilayer MoS<sub>2</sub> transistors with scandium contacts, *Nano Letters*, 13, 100–105, **2012**.
- [28] Fivaz R., Mooser E., Mobility of charge carriers in semiconducting layer structures, *Physical Review*, 163, 743, **1967**.
- [29] Blomquist N., *et al.*, Large-Scale Production of Nanographite by Tube-Shear Exfoliation in Water, *Plosone* 11, e0154686, **2016**.
- [30] Cunningham G., *et al.*, Solvent Exfoliation of Transition Metal Dichalcogenides: Dispersion ability of Exfoliated Nano sheets varies only weakly between Compounds, *ACS Nano*, 6, PMID: 22394330, 3468–3480, **2012**.
- [31] Monajjemi M., Liquid-phase exfoliation (LPE) of graphite towards graphene: An abinitio study, *Journal of Molecular Liquids*, 230, 461–472, **2017**.
- [32] Manne S., Amphiphiles at Interfaces, 226–233, **1997**.
- [33] Manne S., Gaub H.E., Molecular Organization of Surfactants at Solid-Liquid Interfaces. *Science*, 270, 1480–1482, **1995**
- [34] Lee H.P., Progress and trends in inkjet printing technology, *Recent progress in inkjet technologies II*, 1–14 **1998**.
- [35] Laboratories X., Practice of Inkjet Technology, *IMI Europe, Letchworth*, **2010**.
- [36] Casiraghi C., In Spectroscopic Properties of Inorganic and Organometallic Compounds: Techniques, Materials and Applications, *the Royal Society of Chemistry*, 43, 29–56, **2012**
- [37] Israelachvili J.N., Intermolecular and surface forces, Academic press, revised 3rd edn, **2011**.
- [38] Bader R.F.W., Atoms in Molecule: A quantum Theory, *Oxford Univ. press, Oxford*, **1990**.
- [39] Becke A.D., Edgecombe A., simple measure of electron localization in atomic and molecular systems, *The Journal of Chemical Physics*, 92, 9, 5397-5403, **1990**.
- [40] Savin A., Nsper R., Wengert S., Fassler T., ELF: The Electron Localization Function, *Angew. Chem. Int. Ed.Engl.*, 36, 17, 1808-1832, **1997**
- [41] Lu T., Chen F., Multiwfn: A Multifunctional Wavefunction Analyzer, *J. Comp. Chem.*, 33, 580-592, **2012**.
- [42] Monajjemi M., Mohammadian N.T., S-NICS an Aromaticity Criterion for Nano Molecules, *J. Comput. Theor. Nanosci*, 12, 4895-4914, **2015**
- [43] Monajjemi M., Lee V.S., Khaleghian M., Honarparvar B., Mollaamin F., Theoretical Description of Electromagnetic Nonbonded Interactions of Radical, Cationic, and Anionic NH<sub>2</sub>BHNBNH<sub>2</sub> Inside of the B18N18 Nanoring, *J. Phys.Chem C*, 114, 15315, **2010**.
- [44] Monajjemi M., Boggs J.E., A New Generation of BnNn Rings as a Supplement to Boron Nitride Tubes and Cages, *J. Phys. Chem. A*, 117, 1670–1684, **2013**
- [45] Monajjemi M., Non bonded interaction between BnNn (stator) and BN B (rotor) systems: A quantum rotation in IR region, *Chemical Physics*, 425, 29-45, **2013**.
- [46] Monajjemi M., Wayne Jr Robert., Boggs J.E., NMR contour maps as a new parameter of carboxyl's OH groups in amino acids recognition: A reason of tRNA–amino acid conjugation, *Chemical Physics*, 433, 1-11, **2014**.
- [47] Monajjemi M., Quantum investigation of non-bonded interaction between the B15N15 ring and BH<sub>2</sub>NBH<sub>2</sub> (radical, cation, and anion) systems: a nano molecularmotor, *Struct Chem*, 23, 551–580, **2012**
- [48] Monajjemi M., Non-covalent attraction of B2N (2, 0) and repulsion of B2N (+) in the BnNn ring: a quantum rotatory due to an external field, *Theor Chem Acc*, 1668-9, **2015**.

- [49] Monajjemi M., Metal-doped graphene layers composed with boron nitride-graphene as an insulator: a nano-capacitor, *Journal of Molecular Modeling*, 20, 2507, **2014**.
- [50] Monajjemi M., Cell membrane causes the lipid bilayers to behave as variable capacitors: A resonance with self-induction of helical proteins, *Biophysical Chemistry*, 207, 114–127, **2015**.
- [51] Monajjemi M., Mahdavian L., Mollaamin F., Interaction of Na, Mg, Al, Si with carbon nanotube (CNT): NMR and IR study *Russian Journal of Inorganic Chemistry*, 54, 9, 1465-1473, **2009**.
- [52] Elsagh A., Zare K., Monajjemi M., Calculation of the magnetic resonance isotropy tensors of the nucleus of POPC phospholipid bilayers in a cell membrane, *Ukrainian Journal of Ecology*, 8, 1, 165-173, **2018**.
- [53] Monajjemi M., Liquid-phase exfoliation (LPE) of graphite towards graphene: An ab initio study, *Journal of Molecular Liquids*, 230, 461 – 472, **2017**.
- [54] Bagheri S., Monajjemi M., Ziglari A., Bio-Derived material for supporting the efficiency of Sodium-Ion Batteries, *Biointerface research in applied chemistry*, 8, 3, 3241-3246, **2018**.
- [55] Shahriari S., Monajjemi M., Zare K., Penetrating to cell membrane bacteria by the efficiency of various antibiotics (clindamycin, metronidazole, azithromycin, sulfamethoxazole, baxdela, ticarcillin, and clavulanic acid) using S-NICS theory, *Biointerface research in applied chemistry*, 8, 3, 3219-3223, **2018**.
- [56] Madani S M, Monajjemi M, Aghaei H., An application of bio-degradable polymers for electrolyte inside Lithium ion batteries including (m, m) SWCNTs as anodic material, *Biointerface research in applied chemistry*, 8, 3, 3207-3212, **2018**.
- [57] Zakeri, M., Monajjemi, M., Effective molecules of some natural product as antidepressant and antihistamine drugs: A NMR study, *Ukrainian Journal of Ecology*, 8, 2, 255-262, **2018**.
- [58] Shahriari S., Monajjemi M., Zare K., increasing the efficiency of some antibiotics on penetrating bacteria cell membrane, *Ukrainian Journal of Ecology*, 8, 1, 671-679, **2018**.
- [59] SamieiSoofi N., Zare K., Monajjemi M., Study of Gilan's environmental plants & natural products as anti-cancer drugs: S-NICS method, *Ukrainian Journal of Ecology*, 8, 2, 217-224, **2018**.

## 6. ACKNOWLEDGEMENTS

The authors are thankful of INT research center in Ho Chi Minh City of Vietnam for their supports of this work.

© 2018 by the authors. This article is an open access article distributed under the terms and conditions of the Creative Commons Attribution license (<http://creativecommons.org/licenses/by/4.0/>).